*Desalination and Water Treatment*
www.deswater.com

doi: 10.5004/dwt.2017.20671

77 (2017) 105–111
May

# A novel microwave-assisted synthesis of $RuO_2$–$TiO_2$ electrodes with improved chlorine and oxygen evolutions

Tran Le Luu[a], Jiye Kim[b], Jeyong Yoon[b,*]

[a]*Department of Mechatronics and Sensor Systems Technology, Vietnamese German University, Le Lai Street, Hoa Phu Ward, Thu Dau Mot City, Binh Duong Province, Vietnam*
[b]*School of Chemical and Biological Engineering, Seoul National University, Gwanak-gu, Daehak-dong, Seoul 151-742, Korea, Tel. +82-2-880-8941; Fax: +82-2-876-891; email: jeyong@snu.ac.kr (J. Yoon)*

Received 6 October 2016; Accepted 16 December 2016

## ABSTRACT

$RuO_2$–$TiO_2$ electrode now becomes popular in the chlor-alkali industry because of high electrocatalytic and stability with chlorine and oxygen evolutions. Using alternative green method for preparation of $RuO_2$–$TiO_2$ electrode is necessary to reduce the cost, time, increase the electrocatalyst performance, stability, and environmental compatibility. In this study, the Ti/$RuO_2$–$TiO_2$ electrodes were synthesized using sol–gel method under microwave irradiation and investigated for the anodic chlorine and oxygen evolutions. This method can produce small size and uniform distribution of $RuO_2$–$TiO_2$ nanoparticles with mean diameter of 8–10 nm on the big crack size surface, which contributes for the increasing of outer active surface area. The chlorine, oxygen evolution efficiency, and stability comparisons show considerably higher for microwave-assisted electrodes than for those obtained by the conventional heating method. Microwave-assisted sol–gel route has been identified as a novel and powerful method for quick synthesis of $RuO_2$–$TiO_2$ electrodes with excellent chlorine and oxygen evolution performances.

*Keywords:* $RuO_2$; Electrocatalyst; Sol–gel; Microwave; Chlorine; Oxygen evolution

## 1. Introduction

Titanium-based anodes nowadays become very important anodes in the chlor-alkali industry, due to their excellent electrocatalytic activity for the chlorine and oxygen evolutions: low overpotential, low cost, enhanced selectivity, and mechanical and chemical stability [1]. This type of electrodes usually consist of a Ti support coated by noble metal oxides as catalyst or their mixtures with valve metal oxide to prevent corrosion [2]. Mostly, the $RuO_2$–$TiO_2$ binary electrode is used in the practical application [3]. The using of novel green fabrication method to synthesis $RuO_2$–$TiO_2$ electrodes now received a lot of attention in order to enhance the efficiency and the environmental compatibility of this process [4]. Beside this, the electrode stability for a long-time performance also should be considered [5]. Various methods for the synthesis of $RuO_2$–$TiO_2$ electrodes were developed, such as sol–gel [6], thermal decomposition [7], polyol [8], Adams fusion [9], electrodeposition [10], etc. Despite of its extensive use in industry and potential applications, the synthesis of $RuO_2$–$TiO_2$ electrode by a method giving high yield at the expense of less amounts of precursors or in less duration time needs to be considered. In this regard, an approach based on the attractive sol–gel route for the preparation of noble metal oxides seems to be promising in both electrocatalytic and stability with chlorine and oxygen evolutions [11]. The improvement is due to an enlargement of the coating active surface area, increased contribution of the so-called geometric catalytic factor, caused by the formation of finely dispersed oxide particles during the sol–gel procedure. The microwave heating, which is rapid, easy, and energy efficient, has been used for synthesizing of nanomaterials over the last

---

* Corresponding author.

two decades, especially to improve the capacitance of $RuO_2$ for supercapacitors [12–14]. To the best of our knowledge, until now no research about microwave-assisted synthesis of binary $RuO_2$–$TiO_2$ electrode for chlorine and oxygen evolutions are reported yet. In the present study, a novel microwave-assisted synthesis of $RuO_2$–$TiO_2$ electrodes using the sol–gel method is investigated for chlorine and oxygen evolution performances. The physicochemical and electrochemical properties of the obtained electrodes prepared by microwave-assisted are compared with the electrode formed by the conventional heating procedure. The microstructures of as-prepared electrodes are evaluated by scanning electron microscope (SEM), transmission electron microscopy (TEM), and X-ray diffraction (XRD). The electrochemical properties are examined with cyclic voltammetry (CV), linear sweep voltammetry (LSV), total chlorine concentration and accelerated stability test (AST) methods.

## 2. Experimental setup

### 2.1. Electrodes preparation

The preparation of the titanium-coated $RuO_2$–$TiO_2$ electrodes was done using sol–gel method. Titanium foils (dimensional 30 × 20 × 0.25 mm, purity 99.7%, Sigma-Aldrich (St. Louis, Missouri, United States)) were utilized as the substrate materials, of which the contaminants were removed by emery paper, degreased in acetone, and then etched in boiling concentrated hydrochloric acid at 86°C in 1 h to produce gray surface with uniform roughness. A solution containing 40 mM $RuCl_3$, 60 mM $TiCl_3$, 0.2 M $(NH_4)_2CO_3$, 0.1 M $H_2O_2$ (Sigma-Aldrich (St. Louis, Missouri, United States), 99%) were employed as the precursor [15]. The metal ratio Ru:Ti (4:6 mol/mol) chosen depends on the optimization of some previous reports to obtain highest electrocatalytic and stability performances of $RuO_2$–$TiO_2$ electrodes [11]. The pH of the mixture was maintained between 9 and 10. The mixture was treated under microwave irradiation (oven MARS 5, CEM Corporation, USA) with the energy intensities of 400 and 800 W for 20 min at the temperature 80°C [16]. For comparison, conventional $RuO_2$–$TiO_2$ electrode was prepared using classical route by heating the mixture to 80°C for 6 h, with a temperature controlled hot plate. The synthesized metal oxide nanoparticles were separated from solution by centrifugation under 10,000 rpm. The products were then washed with deionized water until free of chloride and then dried at 80°C within 5 h. Weight 3 mg of sol mixtures $RuO_2$–$TiO_2$, dissolved in isopropanol and then coated on the pretreated Ti substrates. Next, the electrodes were sintered at 450°C for 1 h to allow hydrous removal and formation of the metal oxides [17]. Back side of the electrode was covered with epoxy to prevent its exposure to the electrolytes.

### 2.2. Microstructure characterization

The microstructure of the electrode surfaces was characterized by field emission scanning electron microscopy system (JSM-6701F, JEOL Co., Japan). The SEM images were taken at a working distance of 7 mm and an accelerating voltage of 10 kV. The samples were positioned horizontally [18].

Crystal images were examined using a TEM (JEOL 2000EXII, Japan). The TEM samples were prepared by scraping off the coating using a sharp knife and dispersing the powders in isopropyl alcohol. A few drops of these solutions were then deposited on carbon film-coated Cu grids and analyzed with a microscope [19]. The accelerating voltage was 110 kV, the vacuum system was 10 Pa, and tilting angles were ±25°.

In order to study the crystallinity of $RuO_2$ electrode, high resolution XRD pattern was obtained with the grazing incidence technique on a D8 Discover (Bruker-AXS, Germany) diffractometer (Cu $K\alpha$, $\lambda = 1.5406$ Å). A scintillation counter detector scanned between 25° and 100° in $2\theta$ with an angle of incidence was 0.5°, the working distance was 12 mm and the accelerating voltage was 25 kV [20].

### 2.3. Electrochemical measurement and chlorine evolution

The electrochemical characterizations of the $RuO_2$ electrodes with CV and LSV measurements were carried out in a conventional single compartment cell with three electrodes using a computer-controlled potentiostat (PARSTAT 2273A, Princeton Applied Research, USA) [21]. The volume of electrolyte solutions in the cell was 150 mL. $RuO_2$/Ti, Pt (Samsung Chemicals, Korea), and Ag/AgCl (in saturated KCl) were used as the working electrode (anode), the counter electrode (cathode), and the reference electrode, respectively. The CV curves were measured in a solution of 0.5 M $H_2SO_4$ as the electrolyte with the potential ranging between 0 and 1 V and scan rate varying from 5 to 320 mV/s. The voltammetric charge $q$ obtained by integration of the voltammetric curve is a measurement for the number of electrochemically active surface area, which is accessible by the electrolyte. The inner and outer surface areas were identified by plotting and extrapolating the voltammetric charges according to infinitely low (0) and fast (∞) scan rates, which was reported elsewhere [22,23]. The pseudo-capacitive reaction which consists of coupled redox transitions involving proton exchange with the solution at a broad reversible peak around 0.6 V vs. Ag/AgCl can be described as [23]:

$$RuO_x(OH)_y + zH^+ + ze^- \rightarrow RuO_{x-z}(OH)_{y+z} \quad (1)$$

LSV measurements were conducted in the electrolytes containing 5 M NaCl + 0.01 M HCl (pH = 2), which is a favored condition for chlorine evolution and $H_2SO_4$ 1 M with oxygen evolution [2]. The stability of prepared $RuO_2$ electrodes was examined using the AST [24], with a current density considerably higher, and an electrolyte solution more dilute than those usually applied in industrial electrochemical conditions. It provided information about the electrode stability and lifetime (via the electrode potential–time dependence at constant current density). The experiments were performed galvanostatically at the current density of 1 A $cm^{-2}$ in the solution of 0.5 M NaCl, pH = 2 at room temperature (25°C). The $RuO_2$ electrode potential was recorded during the electrolysis.

Chlorine was evolved by electrolysis in a two electrode system with the following condition: an acidic NaCl solution (0.1 M and pH = 2) and a current density 16.7 mA/$cm^2$. The aqueous active chlorine concentration was determined by the *N,N*-diethyl-*p*-phenylenediamine colorimetric method [25]. The experiments were replicated three times and the average value with standard deviation was reported.

## 3. Results and discussion

### 3.1. Chlorine evolution

Fig. 1 shows the difference about chlorine concentrations (a) and LSV (b) of $RuO_2$–$TiO_2$ electrodes made by microwave-assisted and conventional heating method. The chlorine concentrations are higher with the $RuO_2$–$TiO_2$ electrodes prepared by microwave-assisted synthesis method compared with conventional one by the order: convention < MW (microwave)-800 W < MW-400 W. Increase the microwave intensity from 400 to 800 W leads to decrease the chlorine evolution efficiency. The chlorine evolution efficiency increases up to 15.6% in case of microwave-assisted $RuO_2$–$TiO_2$ electrodes compared with the one made by conventional method. The increase of chlorine evolution efficiencies of the $RuO_2$–$TiO_2$ electrodes made by microwave irradiation may be related to the increase of accessible active surface area, which contributes to the electrochemical reaction [26]. The decrease in electrocatalytic activity at high energy intensity may related to the loss of water molecule in $RuO_2$, which favor aggregation process of nanoparticles, leading to decrease in the accessibility for the active surface sites of the catalyst. Clearly, microwave irradiation has a positive role on improving the electrocatalytic performances of $RuO_2$–$TiO_2$ electrodes for chlorine evolution. Chlorine concentrations in Fig. 1(a) are consistent with current density in the region of chlorine evolution measured by LSV, which is shown in Fig. 1(b). At potentials below 1.2 V vs. Ag/AgCl, no reaction takes place. However, potentials exceeding 1.2 V vs. Ag/AgCl cause a steady increase in measured current density, which indicates chlorine formation. The current density in the chlorine evolution region of $RuO_2$–$TiO_2$ electrodes higher with the microwave-assisted synthesis method compared with conventional one.

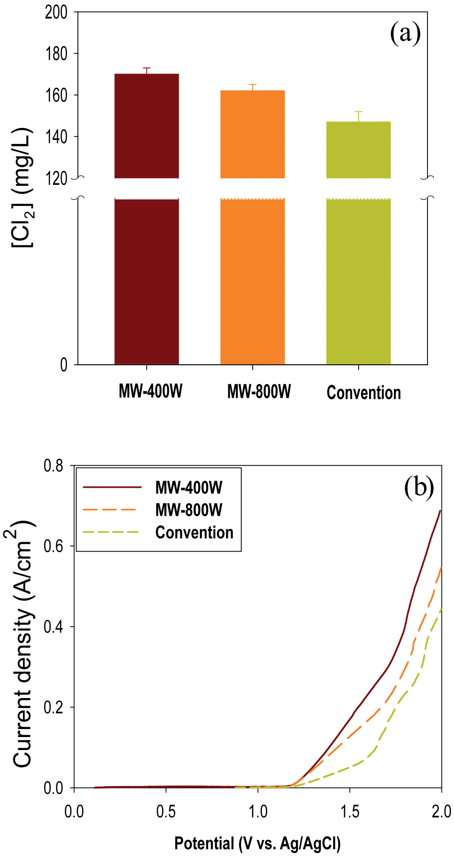

Fig. 1. Chlorine concentrations (a) and LSV (b) of $RuO_2$–$TiO_2$ electrodes made by microwave-assisted and conventional heating methods. Experimental conditions: (a) 0.1 M NaCl, pH = 2, $I$ = 16.7 mA/cm$^2$, $t$ = 10 min; and (b) 5 M NaCl, pH = 2, scan rate = 15 mV/s.

### 3.2. Oxygen evolution

The linear sweep voltammetric patterns of $RuO_2$–$TiO_2$ electrodes made by microwave-assisted and conventional heating methods for oxygen evolution are shown in Fig. 2. At the onset potential 1.0 V vs. Ag/AgCl, oxygen gas start to evolve. All of the electrodes are active with oxygen evolution in the potential range applied, but difference intensity. The current densities of the $RuO_2$–$TiO_2$ electrodes made by microwave route are higher magnitude than the classical one. It is mean that the electrodes with microwave-assisted synthesis also show better catalytic performance with oxygen evolution than the electrode made by conventional heating method. Increase the microwave intensity from 400 to 800 W also leads to decrease the efficiency with the oxygen evolution. The chlorine and oxygen evolution efficiencies of $RuO_2$–$TiO_2$ electrodes seem very consistent with each other. The mechanism of oxygen evolution by metal oxide involves the discharge of the water molecules at the surface to form adsorbed hydroxyl radicals.

This adsorbed hydroxyl radicals are electrochemically oxidized to oxygen or to higher oxide state of the metal, which decompose to yield oxygen [16]. The presence of more active sites on the surface of the metal oxide made by microwave-assisted may determine the better performance of the catalyst toward the anodic oxygen evolution reaction.

### 3.3. Surface analysis

Fig. 3 shows the SEM (a) and TEM (b) images of $RuO_2$–$TiO_2$ electrodes made by microwave-assisted and

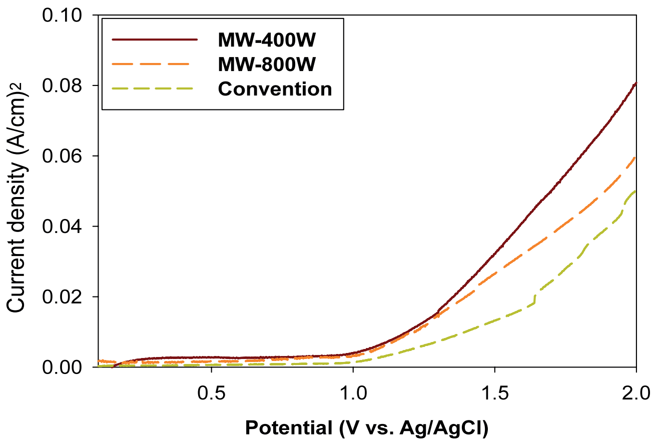

Fig. 2. LSV with oxygen evolutions of $RuO_2$–$TiO_2$ electrodes made by microwave-assisted and conventional methods. Experimental conditions: 1 M $H_2SO_4$, scan rate 10 mV/s.

conventional heating methods. Clearly, the electrode surfaces made by microwave-assisted at energy intensity 400 W, 800 W compared with the conventional heating route are different, which is shown in Fig. 3(a). The morphology of the electrode made by conventional method seem mudcracks (average crack width 1.5 µm) and porous, while the electrodes under microwave synthesis show the bigger crack sizes (average crack width is 2 µm), shaped island-gap and more compact structure, respectively. Each island on the microwave-assisted electrode consists of close-packed catalyst nanoparticles. In this case, the size of the cracks can be regarded as a sort of porosity whose sizes influence mass transfer into the inner part of the catalyst layer and proton exchange during the charge uniform assembly of nanoparticles architecture. The formation of the crack structure is generally attributed to the thermally induced tensile stress during the stage of solvent evaporation. The shrinkage of the xerogel body during the thermal processing is restricted by the underlying Ti substrate. Once the developed stresses exceed the tensile strength of the gel body, cracks develop to release the stress [26].

The homogeneous distribution of nanoparticles is observed from TEM images, which is clearly seen in Fig. 3(b). Due to the annealing temperature, the water molecules in hydrous form are removed and well defined crystals of mixing $RuO_2$–$TiO_2$ are obtained. The crystal size of $RuO_2$–$TiO_2$ nanoparticles made by microwave synthesis shows more uniform and smaller sizes than the electrode made by conventional heating method. The average diameter of $RuO_2$–$TiO_2$ particles with microwave-assisted synthesis at 400 W are in the order of 8–10 nm, while the conventional heating method shows a big range from 15 to 20 nm of particles size. Moreover, the distribution of particle diameter size is bigger when the microwave energy increases (around 12 nm with microwave energy intensity 800 W). This can be attributed to the high energy absorption induce the agglomeration of nanoparticles by reducing its hydrous. It was reported that the absence of structural water may result in the coalescence and growth of $RuO_2$–$TiO_2$ nanoparticles to form larger crystal [16]. The growing of crystal at higher microwave energy is attributed for the reducing of crack size, which is seen in Fig. 3(a). Note that the present of a clearly lattice spacing on certain particulates is $TiO_2$ crystalline. Ti species are relatively concentrated in the central portion, whereas the density of Ru species is slightly higher in the outer portion of this composite although the distributions of both Ti and Ru are uniform. The above results suggest that $RuO_2$ and $TiO_2$ should be formed independently under the sol–gel hydrothermal environment. Because crystalline $TiO_2$ can be formed in aqueous media at room temperature but crystalline $RuO_2$ could only be formed at 80°C under the microwave irradiation or thermal heating. This effect is believed to enhance the exposure of $RuO_2$ in the electrolyte, leading to high $RuO_2$ catalyst utilization [15]. The reduce of crystal size and the increase of crack sizes in the SEM images may increase the outer and total active surface area of the electrodes made by microwave-assisted synthesis than the conventional method. In general, the microwave route produces $RuO_2$–$TiO_2$ nanoparticle can reduce the synthesis time and a better control of the temperature resulting in uniform $RuO_2$–$TiO_2$ nanoparticles, which could induce the higher current density observed in chlorine and oxygen evolutions than the conventional procedure. An understanding of the microwave interaction with materials has been based on concepts of dielectric heating and of the resonance

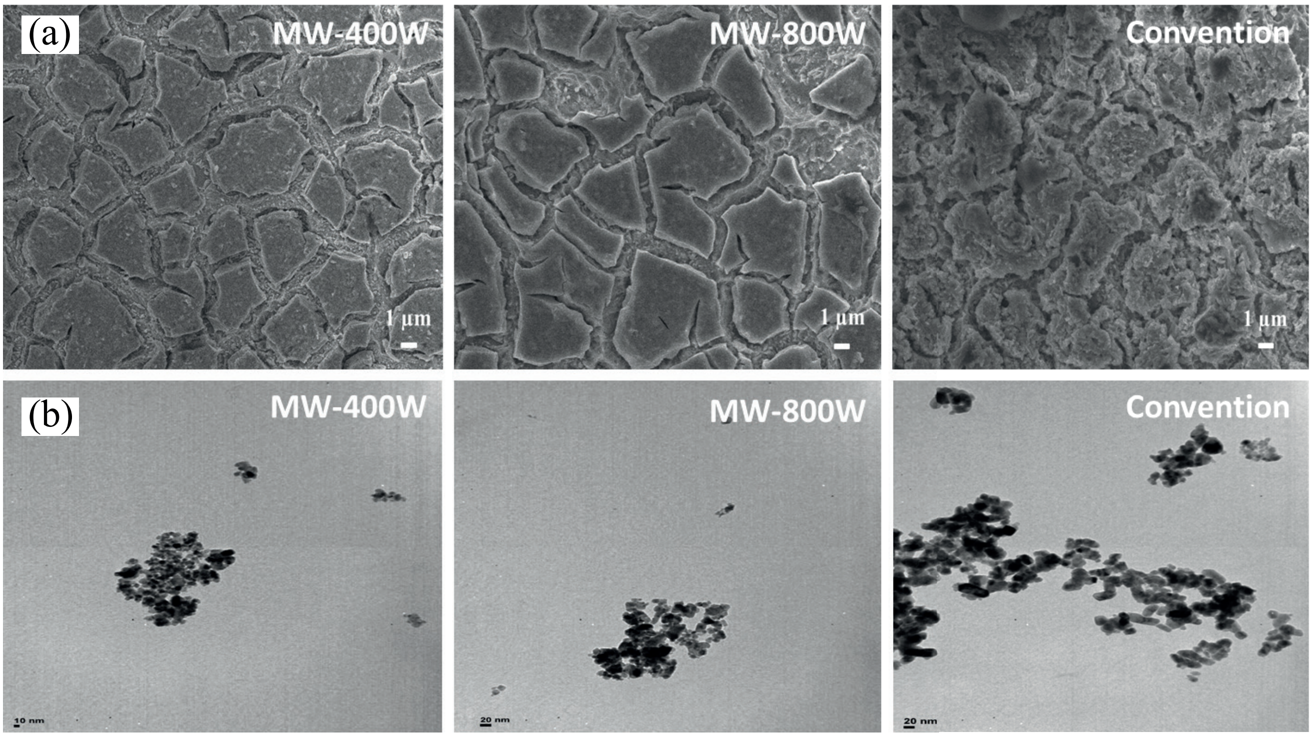

Fig. 3. SEM (a) and TEM (b) images of $RuO_2$–$TiO_2$ electrodes made by microwave-assisted and conventional methods.

absorption due to rotational excitation [12]. The temperature is raised more uniformly throughout whole liquid volume (in-core volumetric heating) under microwave irradiation compared with conventional route is the explanation for this observation.

The diffraction patterns obtained by XRD analysis for $RuO_2$–$TiO_2$ electrodes made by difference microwave energy intensities and conventional heating methods are shown in Fig. 4. The XRD spectra suggest that the oxide nanoparticles in all case are fine and crystalline structure in a set of broad and nearly symmetrical peaks. This indicates the formation of a solid solution, which is desired in terms of electrode stability. The typical peaks of rutile $RuO_2$ metal oxide are easily detected as: 110, 101 planes at about 28° and 35° in all of the electrodes. The most intense peak is 110. Because the catalyst layers are thin, so that X-ray can penetrate through the coating layers and the absorption peaks of Ti metal can be realized. $TiO_2$ metal oxide crystals are presented in both anatase and rutile structures. No evidence of ruthenium metallic phase was observed, which can be found at the higher microwave energy because of ruthenium reduction [27]. The width of the $RuO_2$ peaks from the diffraction profiles show very consistent with the crystal size of the $RuO_2$ nanoparticles measured by TEM images, agrees with Scherrer equation [19].

### 3.4. CV and active surface area

In order to measure the electrochemically active surface area, cyclic voltammetric curves were recorded in the pseudo-capacitive potential range of $RuO_2$–$TiO_2$. Fig. 5 shows the cyclic voltammogram (a) and extrapolated voltammetric charge values (b) from a set of $RuO_2$–$TiO_2$ electrodes. As shown in Fig. 5(a), all CV curves are almost symmetrical to zero potential line. Note that the rectangular shape of the CV of $RuO_2$–$TiO_2$ electrodes remains unchanged with scan rate, indicating the good reversibility (redox reaction) of the system resulting from the insignificant $iR$ (ohmic drop) loss. The currents densities from cyclic voltammograms increase in case of the electrodes made by microwave synthesis than the conventional heating method. But the current density decreases when the microwave energy increase from 400 to 800 W. Fig. 5(b) shows the extrapolated voltammetric charge $q$ values from a set of $RuO_2$–$TiO_2$ electrodes. Since the formations of electrode's morphologies are different, an effect on the total and outer surface area should be visible. The surface area (voltammetric charge) decrease with the increase of scan rate, which mean that the difficulty of the electrolyte to penetrate to the inner surface of the electrode like pore, microcrack, and grain boundary.

The results show that the $q$ values of the total and outer surface area increase with the order of convention < MW-800 W < MW-400 W, respectively. This is very consistent with the current intensities of these electrodes in cyclic voltammograms. The increasing of the crack sizes and decreasing of crystal sizes with the electrodes made by microwave synthesis are the explanation of this order. The total voltammetric charges of microwave-assisted electrodes at 400 W, 800 W are 35.38 mC/cm², 28.92 mC/cm² compared with conventional electrode 26.07 mC/cm². While the value of outer voltammetric charges are 24.86, 22.12, and 15.06 mC/cm², respectively. Microwave-assisted synthesis method can improve

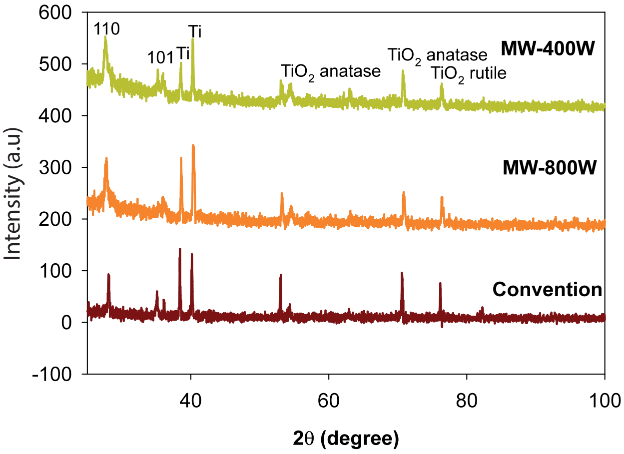

Fig. 4. XRD spectra of $RuO_2$–$TiO_2$ electrodes made by microwave-assisted and conventional methods.

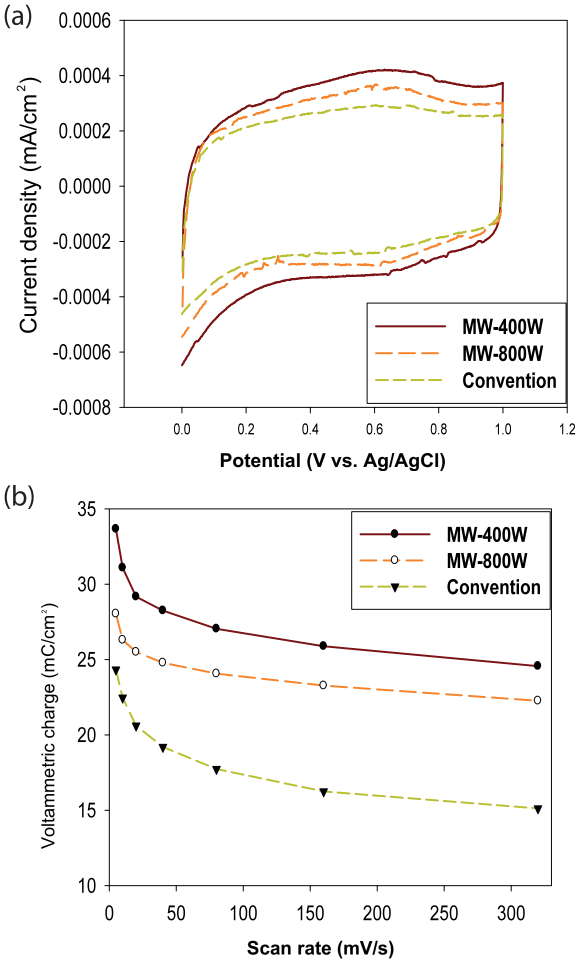

Fig. 5. Cyclic voltammetry (a) in 0.5 M $H_2SO_4$, scan rate 5 mV/s, and charge densities (b) at difference scan rates of $RuO_2$–$TiO_2$ electrodes made by conventional and microwave-assisted methods.

the total and outer surface area of $RuO_2$–$TiO_2$ electrodes compared with the conventional procedure. However, when the microwave energy increases, the total and outer surface areas decrease because of the decreased crack sizes and the increase of crystal sizes. Note that the outer surface area is more important that the total surface area in chlorine evolution [28,29]. The order of oxygen evolution efficiency is convention < MW-800 W < MW-400 W, also match with the increase total charge density of these electrodes. Oxygen evolution efficiency increases with the increasing of total surface area [28]. Microwave irradiation strongly has positive effect to the synthesis process. The electrode made by microwave synthesis shows the higher outer surface area than conventional heating method, so that the oxygen evolution efficiency is higher.

### *3.5. Accelerated stability test*

In the electrochemical production of chlorine, it is undoubtedly the stability that plays the most important role. The sustainability of the electrode's electrocatalytic capability strongly relies on high electrode stability. Vigorous gas evolution takes place in the solution used in the AST. The applied conditions favor oxygen evolution, which makes the investigated coating less stable than under conditions convenient for chlorine evolution [11]. AST supply the fast information about the electrode's stability. The electrode lifetime in the stability test is defined by the time at which the potential of an anode suddenly escalates under galvanostatic conditions in simultaneous oxygen and chlorine evolution reactions. Fig. 5 shows the time dependencies of the electrode potential and the appropriate differential curves for the anodes prepared by the microwave-assisted and conventional heating methods. The lifetime of the $RuO_2$–$TiO_2$ electrodes made by microwave synthesis (up to 230 min) show the longer service life than the electrode made by conventional heating method (150 min). The working life of $RuO_2$–$TiO_2$ electrodes made by microwave at 400 W is longer than 800 W under the same electrolysis condition.

The reason for this observation could either be the larger surface area of the microwave-assisted prepared anodes or the different mechanisms of the catalytic activity loss or both. Two paths for the loss of the electrocatalytic activity have been suggested [11]:

(1) The erosion of the coating: simultaneous electrochemical oxidation of Ru species in the coating forming the soluble products move to the electrolyte.
(2) The penetration of the electrolyte through pores and cracks toward the substrate, which produces insulating $TiO_2$ grains on the interface by oxidation of the substrate.

The morphology of the coating may favor any or all of them together. The oxide particles size is smaller and the distributions are more uniform in the case of the microwave synthesis procedure, which produces a larger surface area than in the conventional method. The smaller nanoparticles sizes help the stronger coalescence and connectivity of each nanoparticle, increase the stability. Consequently, the rate of dissolution of the Ru species on the anode obtained by the microwave-assisted procedure is lower. In the same manner, the structures of the catalytic coating of the microwave synthesis prepared anodes are more compact and penetration of the electrolyte toward the titanium substrate is limited. Then it allows less non-conductive intermediate $TiO_2$ layer formation as compared with the conventional heating anode. Then the erosion of the microwave-assisted electrodes is lower than the conventional heating electrode. It should be noted that the service life mentioned above was obtained in the accelerated life test. Under normal operating conditions (e.g., at current density below 1 A/cm$^2$), the thick electrode would be stable for several years according to many reports [11,25] (Fig. 6).

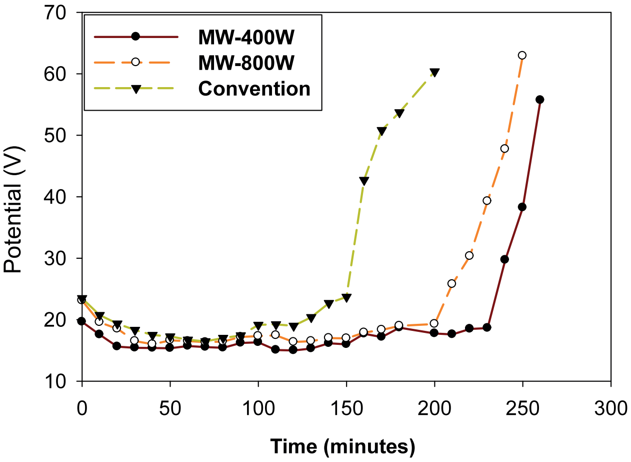

Fig. 6. The AST of $RuO_2$–$TiO_2$ electrodes prepared by the microwave-assisted and conventional heating methods. Experimental conditions: 0.5 M NaCl, pH = 2, $t$ = 25°C, current density = 1 A/cm$^2$.

## 4. Conclusions

The novel microwave-assisted synthesis $RuO_2$–$TiO_2$ electrodes by sol–gel method show considerably higher chlorine, oxygen efficiency, and stability than for those obtained by the conventional heating method. The most important improvement of microwave-assisted synthesis is the increase of outer active surface area compared with the conventional method. Microwave-assisted synthesis method is rapid, clean, cheap, resulting in uniform, small crystalline size, compact structure, and big crack size $RuO_2$–$TiO_2$ nanostructures. Increasing of microwave energy intensity reduces efficiency, stability with oxygen and chorine evolutions because of the increasing crystal size. This research proposes a new approach for synthesis the most popular $RuO_2$–$TiO_2$ electrode for chlor-alkaline industry in the future.

## Acknowledgments

This research was supported by a grant (code 16IFIP-B065893-04) from Industrial Facilities and Infrastructure Research Program funded by Ministry of Land, Infrastructure and Transport of Korean government.

## References

[1] T. Luu, J. Kim, C. Kim, S. Kim, J. Yoon, The effect of fabrication conditions of $RuO_2$ electrode to the chlorine electrocatalytic activity, Bull. Korean Chem. Soc., 36 (2015) 1411–1417.

[2] T. Luu, J. Kim, J. Yoon, Physicochemical properties of $RuO_2$ and $IrO_2$ electrodes affecting chlorine evolutions, J. Ind. Eng. Chem., 21 (2014) 400–404.

[3] J. Osmana, J. Crayston, A. Pratt, D. Richens, $RuO_2$–$TiO_2$ mixed oxides prepared from the hydrolysis of the metal alkoxides, Mater. Chem. Phys., 110 (2008) 256–262.

[4] A. Zeradjanina, F. Mantiab, J. Masaa, W. Schuhmann, Utilization of the catalyst layer of dimensionally stable anodes—interplay of morphology and active surface area, Electrochim. Acta, 82 (2012) 408–414.

[5] L.D. Burke, N.S. Naser, Metastability and electrocatalytic activity of ruthenium dioxide cathode used in water electrolysis cells, J. Appl. Electrochem., 35 (2005) 931–938.

[6] V. Panic, A. Dekanski, M. Stankovic, S. Milonjic, B. Nikoli, On the deactivation mechanisms of $RuO_2$–$TiO_2$/Ti anodes prepared by the sol–gel procedure, J. Electroanal. Chem., 579 (2005) 67–76.

[7] R. Burrows, D. Denton, J. Harrision, Chlorine and oxygen evolution on various compositions of $RuO_2$/$TiO_2$ electrodes, Electrochim. Acta, 23 (1978) 493–500.

[8] A.J. Terezo, E.C. Pereira, Preparation and characterization of Ti/$RuO_2$ anodes obtained by sol–gel and conventional routes, Mater. Lett., 53 (2002) 339–345.

[9] J. Ribeiro, M.S. Moats, A. Andrade, Morphological and electrochemical investigation of $RuO_2$–$Ta_2O_5$ oxide films prepared by the Pechini–Adams method, J. Appl. Electrochem., 38 (2008) 767–775.

[10] C. Hu, C. Wang, T. Wu, K. Chang, Anodic composite deposition of hydrous $RuO_2$–$TiO_2$ nanocomposites for electrochemical capacitors, Electrochim. Acta, 85 (2012) 90–98.

[11] V. Panic, A. Dekanski, S. Milonjic, R. Atanasoski, B. Nikolic, $RuO_2$–$TiO_2$ coated titanium anodes obtained by the sol–gel procedure and their electrochemical behaviour in the chlorine evolution reaction, Colloids Surf., A, 157 (1999) 269–274.

[12] I. Bilecka, M. Niederberger, Microwave chemistry for inorganic nanomaterials synthesis, Nanoscale, 2 (2010) 1358–1374.

[13] J. Kim, K. Kim, S. Park, K. Kim, Microwave-polyol synthesis of nanocrystalline ruthenium oxide nanoparticles on carbon nanotubes for electrochemical capacitors, Electrochim. Acta, 55 (2010) 8056–8061.

[14] S. Yan, H. Wang, P. Qu, Y. Zhang, Z. Xiao, $RuO_2$/carbon nanotubes composites synthesized by microwave-assisted method for electrochemical supercapacitor, Synth. Met., 159 (2009) 158–161.

[15] C. Hu, Y. Yang, T. Lee, Microwave-assisted hydrothermal synthesis of $RuO_2.xH_2O$–$TiO_2$, nanocomposites for high power supercapacitors, Electrochem. Solid-State Lett., 13 (2010) 173–176.

[16] A. Devadas, S. Baranton, T. Napporn, C. Coutanceau, Tailoring of $RuO_2$ nanoparticles by microwave assisted “Instant method” for energy storage applications, J. Power Sources, 196 (2011) 4044–4053.

[17] R. Kotz, S. Stuck, Stabilization of $RuO_2$ by $IrO_2$ for anodic oxygen evolution in acid media, Electrochim. Acta, 31 (1986) 1311–1316.

[18] J. Jirkovsky, H. Hoffmannova, M. Klementova, P. Krtil, Particle size dependence of the electrocatalytic activity of nanocrystalline $RuO_2$ electrodes, J. Electrochem. Soc., 153 (2006) 111–118.

[19] C. Malmgren, A.K. Eriksson, A. Cornell, J. Backtrom, S. Eriksson, H. Olin, Nanocrystallinity in $RuO_2$ coatings—influence of precursor and preparation temperature, Thin Solid Films, 518 (2010) 3615–3618.

[20] H.P. Klug, L.E. Alexander, X-Ray Diffraction Procedures, 2nd ed., Wiley, New York, 1974.

[21] A. Bard, L. Faulkner, Electrochemical Methods: Fundamentals and Applications, 2nd ed., Wiley, 2001, pp. 200–217.

[22] J. Jeong, C. Kim, J. Yoon, The effect of electrode material on the generation of oxidants and microbial inactivation in the electrochemical disinfection processes, Water Res., 43 (2009) 895–901.

[23] S. Ardizzone, G. Fregonara, S. Trasatti, “Inner” and “outer” active surface of $RuO_2$ electrodes, Electrochim. Acta, 35 (1990) 263–267.

[24] J. Ribeiro, A. Andrade, Microstructure, morphology and electrochemical investigation characterization of $RuO_2$-$Ta_2O_5$ coated titanium electrode, J. Electrochem. Soc., 151 (2004) 106–112.

[25] APHA, Standard Methods for the Examination of Water and Wastewater, 21st ed., American Public Health Association, Washington, D.C., USA, 2005, pp. 4–46.

[26] R. Chen, V. Trieu, A.R. Zeradjanin, H. Natter, D. Teschner, J. Kintrup, A. Bulan, W. Schuhmann, R. Hempelmann, Microstructural impact of anodic coatings on the electrochemical chlorine evolution reaction, Phys. Chem. Chem. Phys., 14 (2012) 7392–7399.

[27] J. Sullivan, D. Worsley, Evolution and fractal growth of micro/nano structured wires of ruthenium synthesised by microwave irradiation of ruthenium dioxide, Mater. Lett., 63 (2009) 2335–2338.

[28] L.D. Burke, J.F. O’Neill, Some aspects of the chlorine evolution reaction at ruthenium dioxides anodes, J. Electroanal. Chem. Interfacial Electrochem., 101 (1979) 341–349.

[29] S. Trasatti, Progress in the understanding of the mechanism of chlorine evolution at oxide electrodes, Electrochim. Acta. 32 (1987) 369–382.